Pharmaceutical Research, Vol. 22, No. 5, May 2005 (© 2005)
DOI: 10.1007/s11095-005-2597-4

Research Paper

Comparison of Molecular Mobility in the Glassy State Between Amorphous Indomethacin and Salicin Based on Spin-Lattice Relaxation Times

Katsuhiko Masuda,[1,2,6] Sachio Tabata,[3] Yasuyuki Sakata,[4] Tetsuo Hayase,[5] Etsuo Yonemochi,[1] and Katsuhide Terada[1]

Received May 17, 2004; accepted January 26, 2005

Purpose. The purpose of the current study was to evaluate the molecular mobility of amorphous indomethacin and salicin in the relaxed glassy state based on spin-lattice relaxation times (T_{1c}) and to clarify the effects of molecular mobility on their physical stability.
Methods. Pulverized glassy amorphous indomethacin and salicin samples were completely relaxed, and the T_{1c} values were investigated using solid-state ^{13}C-nuclear magnetic resonance (NMR) at temperatures below the glass transition temperature (T_g). All NMR spectra were obtained using the T_{1c} measurement method combined with variable-amplitude cross-polarization, the Torchia method, and total sideband suppression method.
Results. The T_{1c} value of amorphous indomethacin indicated that 73% of carbons were in a state of monodispersive relaxation, suggesting that the amorphous state was relatively homogeneous and restricted, particularly in backbone carbons. On the other hand, 92% of carbons of amorphous salicin exhibited both fast and slow biphasic relaxation. Individual structures of the salicin molecules behaved heterogeneously, and thus the entire molecule showed relatively fast local as well as slow mobility.
Conclusions. At temperatures below T_g, amorphous salicin had relatively greater molecular mobility than amorphous indomethacin. This difference in the molecular mobility of the two compounds is correlated with their crystallization behavior. Solid-state ^{13}C NMR provides valuable information on the physical stability of amorphous pharmaceuticals.

KEY WORDS: amorphous indomethacin; amorphous salicin; molecular mobility; solid-state ^{13}C NMR; spin-lattice relaxation times (T_{1c}).

INTRODUCTION

The amorphous forms of various pharmaceutical compounds have been investigated in attempts to improve their dissolution rates and bioavailability (1). Many amorphous compounds, however, are chemically and physically unstable compared with their crystal forms due to the greater degree of molecular mobility in the amorphous state relative to the crystalline state. A critical parameter for characterizing the amorphous state is the glass transition temperature (T_g). We do not yet have a detailed understanding of the relationship between the molecular mobility and stability of amorphous pharmaceuticals, especially below T_g. Numerous studies have been performed on the physical stability of amorphous materials in terms of molecular mobility and thermodynamic quantities at temperatures below T_g (2–14).

It is important to clarify the relationship between the molecular mobility and crystallization rate of amorphous pharmaceuticals. It is generally recognized that mass transport is the most pivotal factor in nucleation and crystal growth from the very viscous amorphous state. It was reported that the crystallization rate from amorphous solids at temperature T depends on the rate of molecular diffusion across the nuclear-amorphous interface, D(T), and the nucleation free energy, f(T) (11). Therefore it is reasonable to study the physical stability of amorphous pharmaceuticals based on their molecular mobility. The molecular mobility of amorphous pharmaceuticals has been demonstrated in dynamic mechanical analyses using shear viscosity measurement, ^1H pulse nuclear magnetic relaxation, differential scanning calorimetry, and isothermal microcalorimetry. Yu (1), Sillescu (8), and Ediger *et al.* (12) reviewed the theories and various experimental methodologies for determining the molecular mobility of amorphous materials. Based on shear viscosity measurements, Andronis and Zografi (15) reported that a high degree of molecular mobility occurs in amorphous indomethacin at temperatures near T_g. The molecular mobility obtained in viscosity measurements shows a non-Arrhenius temperature dependence with the apparent activation energies of the order 220 KJ/mol at around T_g. Aso *et al.* (16)

[1] Department of Pharmaceutics, Toho University School of Pharmaceutical Sciences, Funabashi, Chiba, Japan.
[2] Discovery Technology Laboratory II, Mitsubishi Pharma Corporation, Aoba-ku, Yokohama, Kanagawa, Japan.
[3] Yokohama Laboratory, Mitsubishi Chemical Group Science and Technology Research Center, Inc., Aoba-ku, Yokohama, Kanagawa, Japan.
[4] Yokkaichi Laboratory, Mitsubishi Chemical Group Science and Technology Research Center, Inc., Toho-cho, Yokkaichi, Mie, Japan.
[5] Pharmaceutical Technology Coordination Department, Mitsubishi Pharma Corporation, Hasaki Kashima, Ibaraki, Japan.
[6] To whom correspondence should be addressed (e-mail: Masuda.Katsuhiko@mk.m-pharama.co.jp)

assessed the molecular mobility of amorphous nifedipine, phenobarbital, and flopropione using both ^{1}H pulse nuclear magnetic relaxation and enthalpy relaxation and found that amorphous nifedipine has greater molecular mobility than amorphous phenobarbital and flopropione at temperatures lower than T_g. This observation correlates with the more rapid crystallization of nifedipine compared with that of phenobarbital or flopropione.

The changes in specific volume or enthalpy that generally occur in glassy samples are shown in Fig. 1. A freshly prepared glassy sample (glass 1 in Fig. 1) moves toward the more quasi-equilibrium glassy state (glass 2), with decreases in enthalpy and specific volume (4) in a process known as enthalpy relaxation. Most studies of the molecular mobility of glassy samples focused on the enthalpy relaxation process. Andronis and Zografi (13) pointed out that after an amorphous compound is fully relaxed in the equilibrium state, detectable crystallization occurs, as depicted by the movement of glass 2 to the crystalline state in Fig. 1. The enthalpy relaxation time and crystallization rate of glassy-state indomethacin are approximately 1 h at 303 K and more than 80 days at room temperature (17), respectively, and those of glassy salicin are 30 h at 303 K (unpublished data) and 12 days at room temperature (18), respectively. Thus, it can be assumed that after the enthalpy relaxation period, a glassy amorphous compound still has molecular mobility.

Few studies have been performed on the molecular mobility of amorphous compounds after enthalpy relaxation. ^{13}C nuclear magnetic relaxation times not only provide information on the molecular mobility of individual structures in molecules, but also on the entire molecule after enthalpy relaxation. Although some reports are available on amorphous pharmaceutical compounds using ^{13}C nuclear magnetic relaxation times (11,19), they are limited to the enthalpy relaxation process.

The purpose of this study was to investigate the differing mobility of each functional group in the molecules of amorphous pharmaceutical compounds using indomethacin and salicin as models. The mobility of each functional group was evaluated based on the spin-lattice relaxation times (T_{1c}) using solid-state ^{13}C nuclear magnetic resonance (NMR) after the enthalpy relaxation period. The molecular mobility of the two compounds in the amorphous state was compared.

MATERIALS AND METHODS

Materials

Crystalline indomethacin (1-(*p*-chlorobenzoyl)-5-methoxy-2-methylindole-3-acetic acid) and salicin (2-(hydroxymethyl)phenyl-β-D-glucopyranoside) were purchased from Sigma Chemical (St. Louis, MO, USA) and used as received. Amorphous materials were prepared by heating the indomethacin and salicin to the melting point in a reservoir for approximately 10 min, followed by quenching in liquid nitrogen. The chemical degradation of the pharmaceuticals was negligible during the preparation process and storage of amorphous samples.

The glassy samples were gently pulverized in a mortar and placed in solid-state NMR sample holders under a dry plastic container to prevent moisture uptake from room air. Before solid-state ^{13}C NMR measurement, the samples were stored under dry conditions for 2 days.

Methods

T_{1c} Measurement of Amorphous Pharmaceuticals

Solid-state ^{13}C NMR spectra were recorded using a Chemagnetics CMX-400 spectrometer (Fort Collins, CO, USA) operating at a carbon frequency of 100.56 MHz. The amorphous indomethacin and salicin samples were spun by a jet of dry air at the magic angle (54.7°) with a spinning rate of 5 and 11 kHz in the 7.5- and 4-mm ϕ internal diameter probe head, respectively. All spectra were obtained using the T_{1c} measurement method combined with variable-amplitude cross

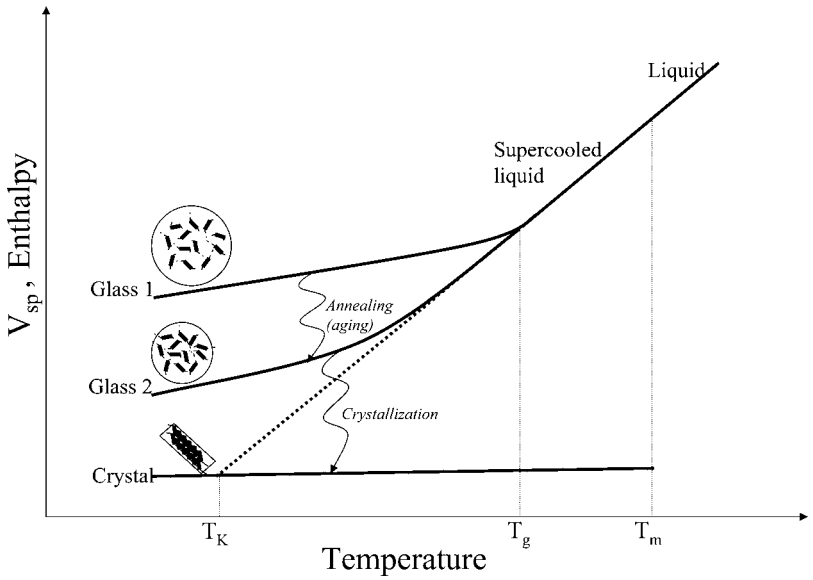

Fig. 1. Schematic representation of the change in specific volume (V_{sp}) and enthalpy (H) as a function of temperature for a vitrifying and crystallizing material. (T_K: Kauzman temperature; T_g: glass transition temperature; T_m: melting temperature.) Partially modified from Ref. 4 (J. Liu *et al. J. Pharm. Sci.*, **91**:1853 (2002)).

polarization, the Torchia method (20), and total side-band suppression method (21). The contact times were 4 ms and 1 ms, and the pulse delays between scans were 12 s and 10 s for amorphous indomethacin and salicin, respectively. All spectra were recorded at 281 K (T_g – 40 K) and 293 K (T_g – 40 K) for amorphous indomethacin and salicin, respectively. The chemical shifts were externally referenced to the methylene signal of adamantane at 38.52 ppm.

T_{1c} Calculations

Generally, the magnetic relaxation phenomenon can be expressed by an index function of the decay type. Hence the T_{1c} values were estimated using a nonlinear least-square fitter with the Levenberg-Marquardt algorithm on Origin ver. 6J (Microcal Software, Inc., Northampton, MA, USA). Equation (1) was derived after fitting by plotting relaxation delay times (τ) vs. signal heights of the solid-state ^{13}C NMR spectra. All fittings were accomplished by minimizing the sum of squared deviation between the observed and calculated values using repeated calculations in the Lagrange multiplier method (22) under the condition that $T_{1c} > 0.1$ s.

$$M_\tau = M_0 \exp\left(-\frac{\tau}{T_1}\right) \tag{1}$$

where M_τ is the signal height of the solid-state ^{13}C NMR spectrum at each relaxation delay time (τ), M_0 is the signal height of the solid-state ^{13}C NMR spectrum when τ is zero, and T_1 is the magnetic relaxation time. The calculation range of τ was selected based on the signal-to-noise ratio of solid-state ^{13}C NMR spectra.

When the values calculated using Eq. (1) approximately agreed with the observed values [i.e., the value of the coefficient of determination (R^2) was greater than 0.990], the solid-state ^{13}C NMR signal was considered to have magnetic relaxation in the monodispersive mode, even when solid-state ^{13}C NMR signals overlapped in the spectra. On the other hand, if the relaxation behavior of a ^{13}C NMR signal could not be expressed by Eq. (1), the signal was considered to have magnetic relaxation in the multidispersive mode.

In these cases, a composite function of Eq. (1) can be approximated, as theoretically shown in Eq. (2), to represent $T_{1(i)}$.

$$M_\tau = M_{0(1)}\exp\left(-\frac{\tau}{T_{1(1)}}\right) + M_{0(2)}\exp\left(-\frac{\tau}{T_{1(2)}}\right) + M_{0(3)}\exp\left(-\frac{\tau}{T_{1(3)}}\right) + \cdots + M_{0(n)}\exp\left(-\frac{\tau}{T_{1(n)}}\right) \tag{2}$$

In this study, Eq. (2) can be expressed as a two-phase model by Eq. (3) when it can be assumed that the solid-state ^{13}C NMR signal has both long and short magnetic relaxation times.

$$M_\tau = M_{0(1)}\exp\left(-\frac{\tau}{T_{1(1)}}\right) + M_{0(2)}\exp\left(-\frac{\tau}{T_{1(2)}}\right) \tag{3}$$

When the magnetic relaxation is in the multidispersive mode, and the values calculated from Eq. (3) approximately agree with the observed data (i.e., the value of R^2 is greater than 0.990), it is considered that the solid-state ^{13}C NMR

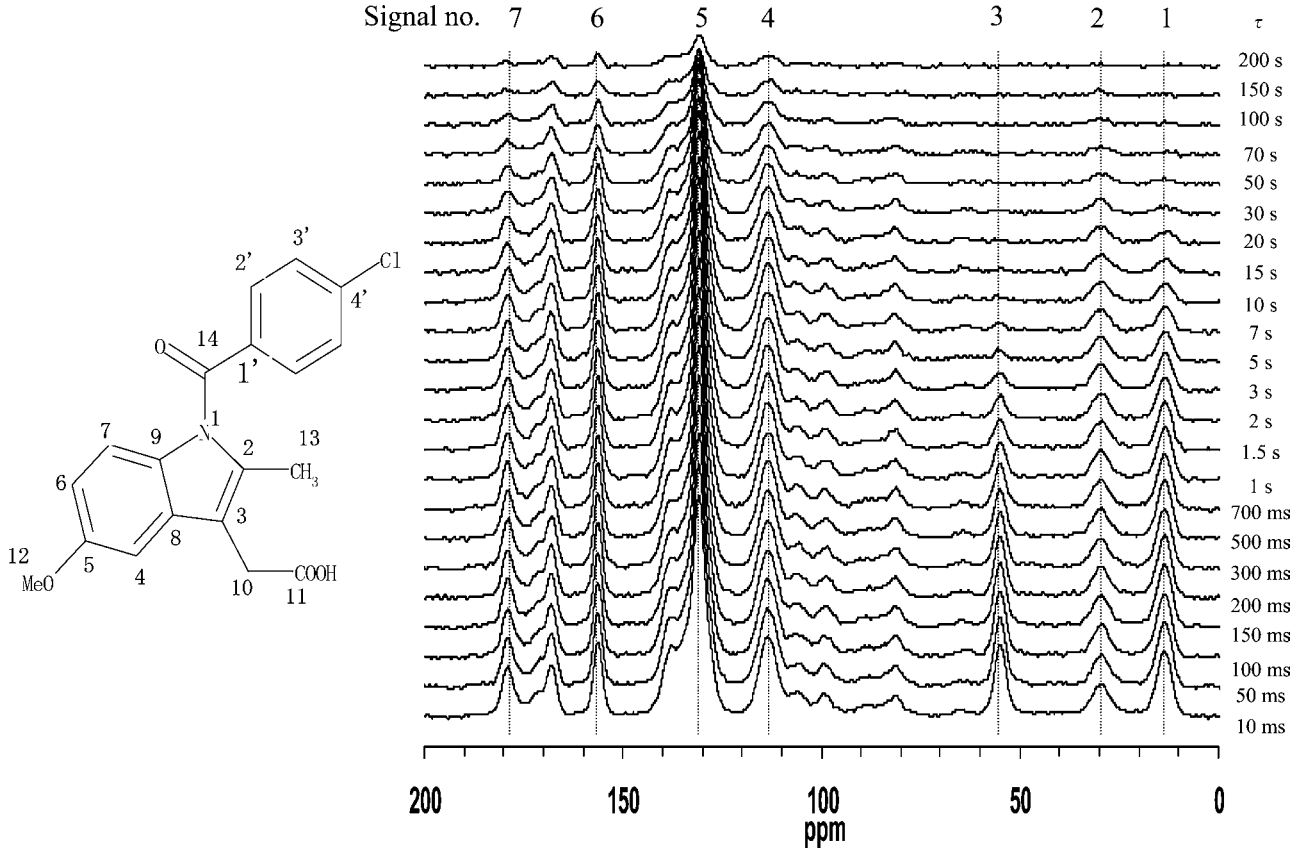

Fig. 2. Solid-state ^{13}C NMR spectra of amorphous indomethacin.

Table I. Magnetic Relaxation Times (T_{1c}) of Amorphous Indomethacin at 281 K (40 K lower than T_g)

Signal no.	Chemical shift (ppm) Solid-state	Chemical shift (ppm) Solution [d4-methanol]	Carbon no.	Magnetic relaxation mode	T_{1c} (s) Shorter	T_{1c} (s) Longer
1	13.7	13.6	13	Multidispersive	2.6	18
2	29.3	30.7	10	Multidispersive	5.7	81
3	55.0	56.3	12	Multidispersive	0.8	4.8
4	113.5	112.8–116.0	3, 6, 7	Monodispersive	76	
5	130.9	130.4–140.3	1′–4′, 2, 8, 9	Monodispersive	85	
6	156.3	157.8	5	Monodispersive	77	
7	178.9	175.1	11	Multidispersive	9.8	94

signal is represented by the two-phase model and consists of both long T_{1c} and short T_{1c}. Other calculation conditions used were the same as those for magnetic relaxation in the monodispersive mode.

RESULTS AND DISCUSSION

Molecular Mobility of Indomethacin

Figure 2 shows typical solid-state ^{13}C NMR spectra of amorphous indomethacin recorded using the T_{1c} measurement pulse sequence. The spectral patterns showed broad signals for typical amorphous material. If crystallization had occurred, sharp signals should have been detected. In addition, to confirm that crystallization did not occur during this experiment, amorphous indomethacin was stored at 281 K, 40 K lower than T_g, and analyzed using X-ray diffraction. No crystallization was detected in the X-ray diffraction pattern of stored sample.

Spectral assignments for the solid-state spectra, based on the original solution-phase NMR assignments in distortionless enhancement polarization transfer, heteronuclear single-quantum coherence (HSQC), and heteronuclear multiple-

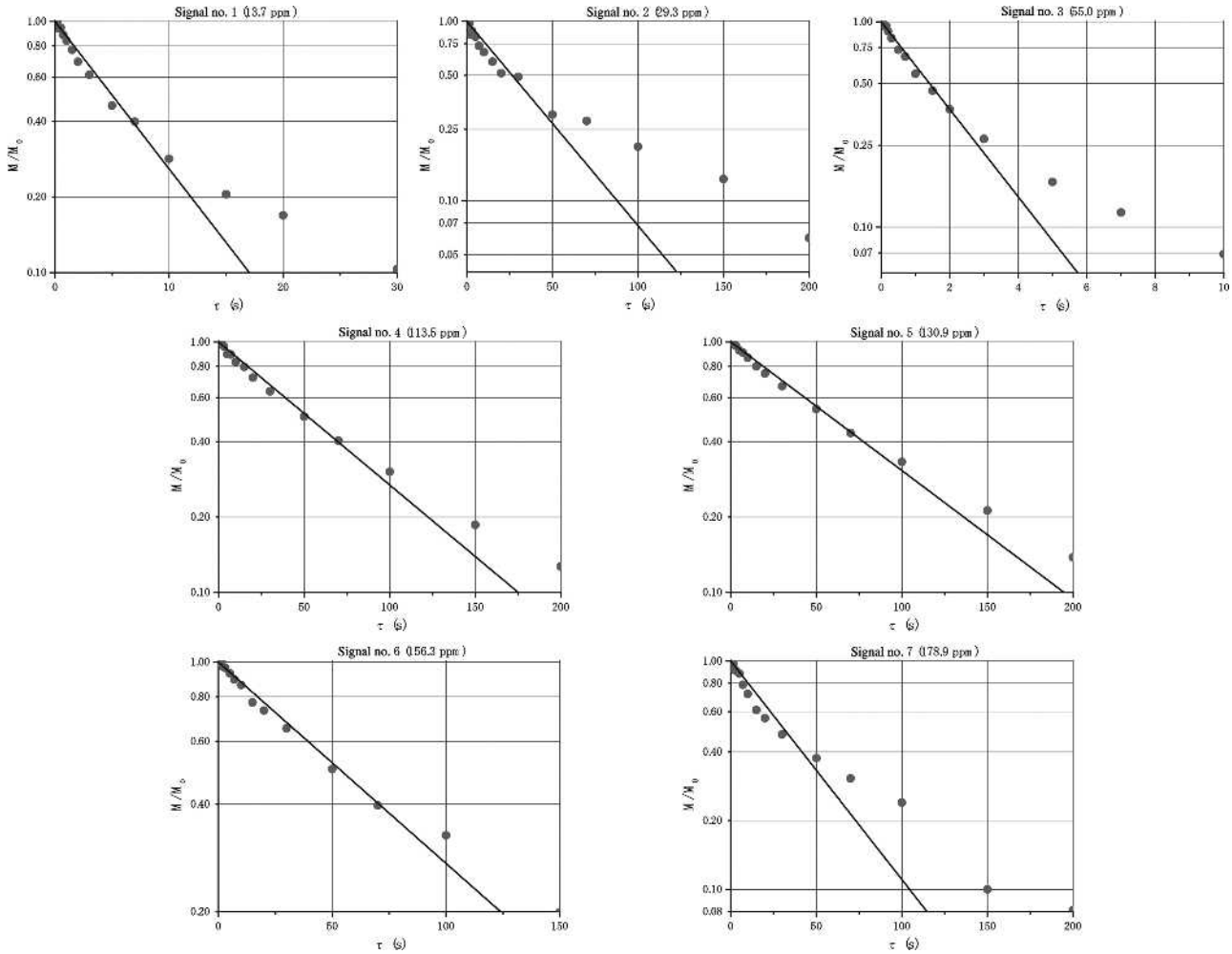

Fig. 3. Relaxation delay time (τ) vs. M_τ/M_0 for amorphous indomethacin. The solid line is the fit to Eq. (1).

bond connectivity (HMBC) spectroscopy, are presented in Table I. Figure 3 shows spin-lattice relaxation processes observed at 281 K, which is 40 K lower than the T_g. The M_τ/M_0 value of each signal of amorphous indomethacin was calculated against τ using the monodispersive relaxation mode of Eq. (1). It was confirmed that the observed values for signals 4, 5, and 6 fit the calculated curves well (i.e., the R^2 values were 0.990, 0.993, and 0.990, respectively). This result indicates that signals 4, 5, and 6 were consistent with the monodispersive relaxation mode, even though one signal was attributed to several carbons (i.e., signal 5 was attributed to carbon numbers 1′, 2′, 3′, 4′, 2, 8, and 9 shown in Fig. 2). On the other hand, signals 1, 2, 3, and 7 did not fit the monodispersive relaxation mode, although they could be fitted to the multidispersive relaxation curve using Eq. (3). The relaxations of these signals were expressed by two T_{1c} values, the longer and shorter T_{1c}, as shown in Fig. 4 (i.e., the R^2 values were 0.998, 0.991, 0.999, and 0.997, respectively). The T_{1c} values for each peak of amorphous indomethacin are summarized in Table I. The T_{1c} values for signals 1, 2, 3, and 7, which are due to the side chain carbons 10, 11, 12, and 13 in Fig. 1, were observed to be in the multidispersive mode, while T_{1c} values for signals 4, 5, and 6, which are attributed to the carbons of the indole ring and phenyl ring (carbon numbers 1'–4', 2, 3, 5, 6, 7, 8, and 9 in Fig. 2), were observed to be in the monodispersive mode. These phenomena suggest that amorphous indomethacin molecules do not exhibit homogeneous mobility.

The T_{1c} values for signals 4, 5, and 6 were 76–85 s in the monodispersive mode. Because a longer T_{1c} indicates slower molecular mobility of amorphous molecules in solid-state NMR (23), the mobility of the backbone structure composed of the indole ring and phenyl ring of amorphous indomethacin could be described as a slow rotation. In contrast, the relaxation behavior of signals 1, 2, 3, and 7, which are due to the side chain carbons of amorphous indomethacin, was in the multidispersive mode. This should indicate that the side chain of amorphous indomethacin could be rotated around the single bonds in a heterogeneous manner with biphasic relaxation. Because the shorter T_{1c} implies greater molecular mobility, the relatively faster molecular motion of the side chains of amorphous indomethacin was confirmed below T_g at 281 K (40 K lower than T_g). In contrast, the molecular mobility of the indole ring and phenyl ring carbons, which are the backbone structure of indomethacin, was relatively slow and homogeneous compared with that of the side chain carbons. It should be emphasized that the molecular mobility in the backbone structure was restricted; on the other hand, the molecular mobility of the side chain was relatively free in amorphous molecules of indomethacin.

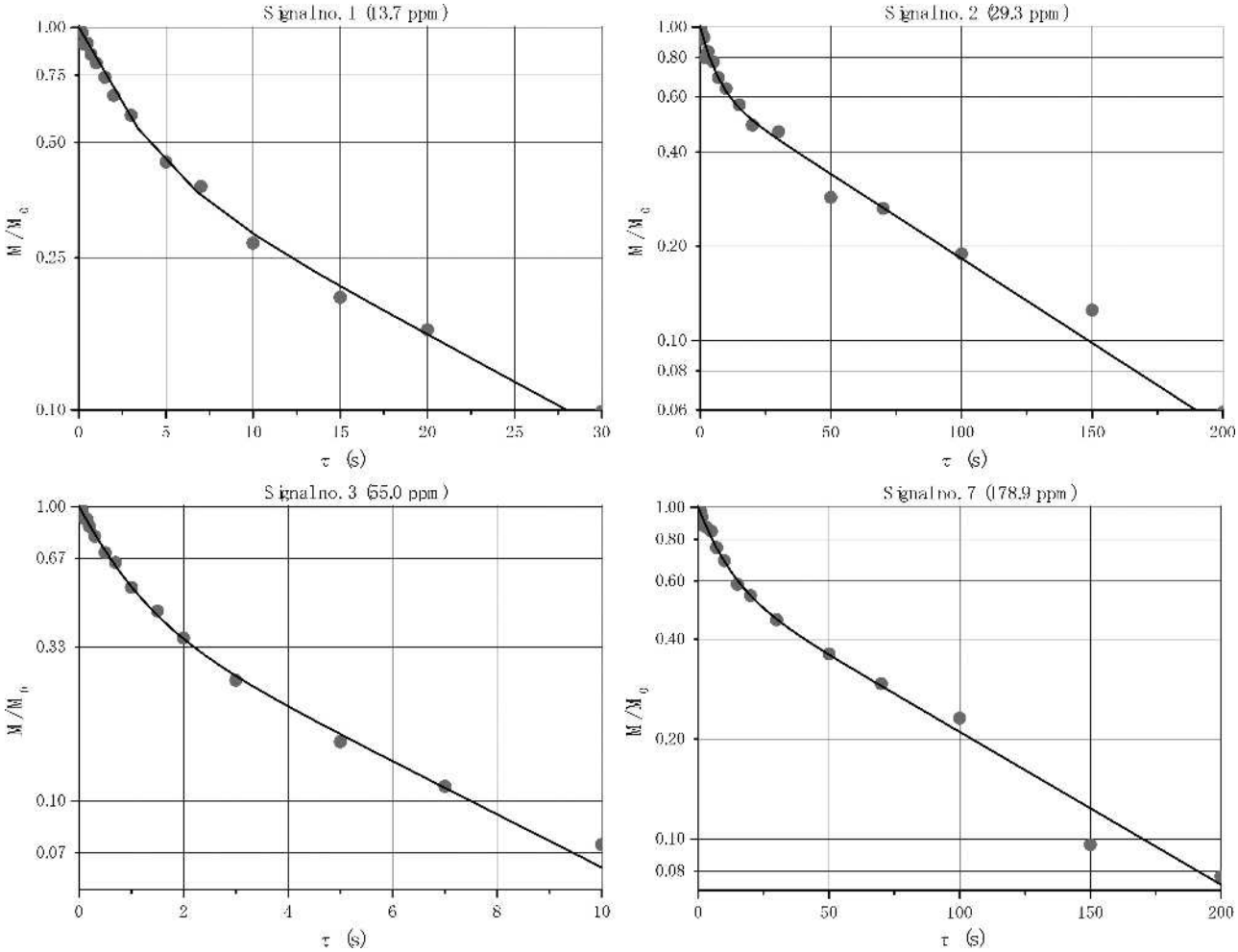

Fig. 4. Relaxation delay time (τ) vs. M_τ/M_0 for signals 1, 2, 3, and 7 of amorphous indomethacin. The solid line is the fit to Eq. (3).

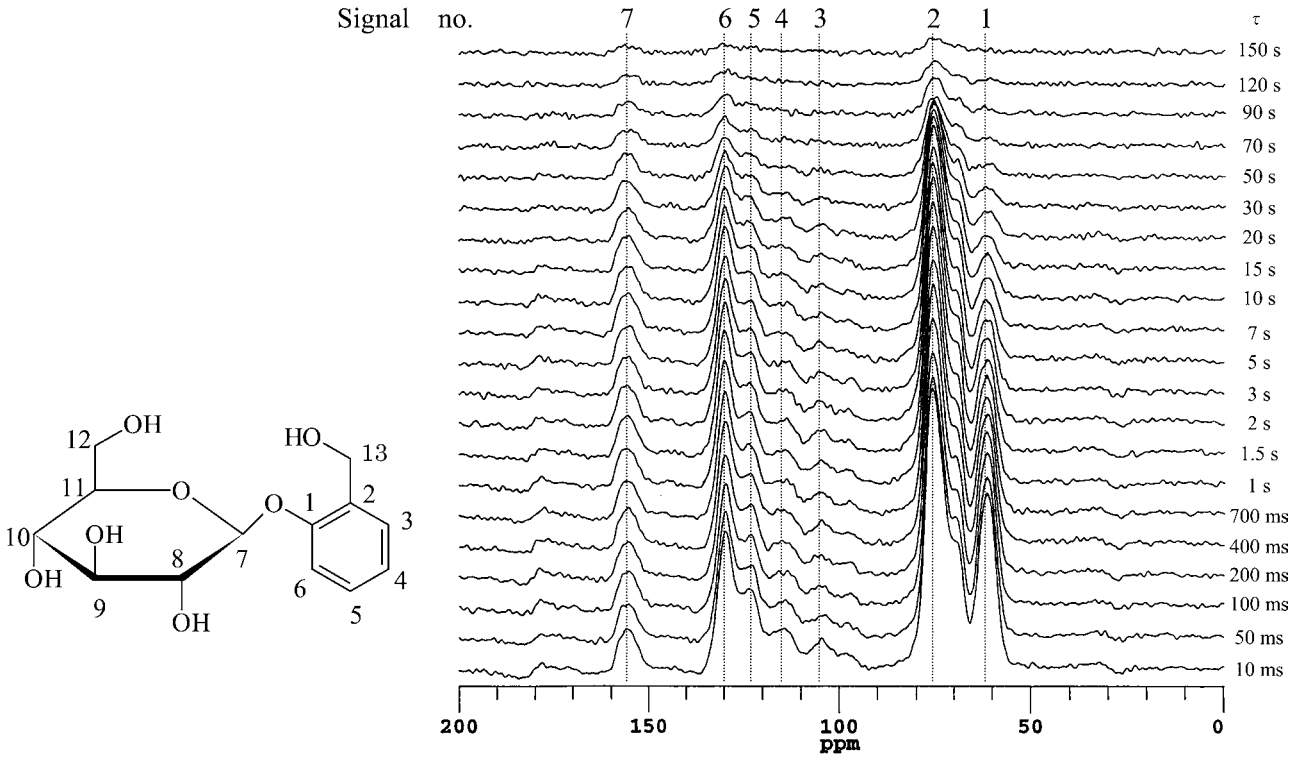

Fig. 5. Solid-state ^{13}C NMR spectra of amorphous salicin.

Molecular Mobility of Salicin

Figure 5 shows typical solid-state ^{13}C NMR spectra of amorphous salicin recorded with T_{1c} measurement pulse sequences. The spectral patterns showed broad signals typical of amorphous material. In a similar manner as the indomethacin samples, amorphous salicin samples were stored at 293 K, and X-ray diffraction analysis was confirmed that no crystallization had occurred.

Spectral assignments for the solid-state spectra, based on the original solution-phase NMR assignments of HSQC and HMBC, are presented in Table II. Figure 6 shows the spin-lattice relaxation process observed at 293 K, which is 40 K lower than T_g. The fitting of M_τ/M_0 for each signal of amorphous salicin was performed using the monodispersive relaxation mode of Eq. (1). As shown in Fig. 6, only signal 7 was fitted to Eq. (1) (i.e., the value of R^2 was 0.990). This result indicates that signal 7 was consistent with the monodispersive relaxation mode. On the other hand, since signals 1, 2, 3, 4, 5, and 6 were not expressed by the monodispersive mode, these signals were analyzed in the multidispersive relaxation mode using Eq. (3). As shown in Fig. 7, signals 2, 3, 4, 5, and 6 were in good agreement with the simulated curves using Eq. (3), with two relaxation modes, and the R^2 values were 0.997, 0.991, 0.991, 0.995, and 0.995, respectively. This also indicates that the relaxation of salicin did not occur in a homogeneous manner.

The T_{1c} values of each peak for amorphous salicin are summarized in Table II. The T_{1c} values for signals 2, 3, 4, 5, and 6 revealed that the samples exhibit multidispersive biphasic fast (about 10 s) and slow (60–78 s) relaxation. Signals 3, 4, and 5 were assigned to single carbons (7, 6, and 4 in Fig. 5), which showed both fast and slow molecular mobility. Signals 2 and 6 were attributed to several carbons (i.e., signal 2 is attributed to carbon numbers 8, 9, 10, and 11 in Fig. 5). In the latter case, it was difficult to determine the molecular mobility

Table II. The Magnetic Relaxation Times (T_{1c}) of Amorphous Salicin at 293 K (40 K lower than T_g)

Signal no.	Chemical shift (ppm)		Carbon no.	Magnetic relaxation mode	T_{1c} (s)	
	Solid-state	Solution [d6-Dimethyl Sulfoxide]			Shorter	Longer
1	61.8	58.4–60.9	12, 13	Multidispersive	n/a	
2	76.1	69.8–77.1	8–11	Multidispersive	12	60
3	105.0	101.5	7	Multidispersive	5.3	65
4	114.6	114.9	6	Multidispersive	14	78
5	123.8	121.8	4	Multidispersive	13	66
6	129.8	127.3–131.6	2, 3, 5	Multidispersive	16	72
7	155.9	154.8	1	Monodispersive	84	

n/a, not fitted by Eq. (3).

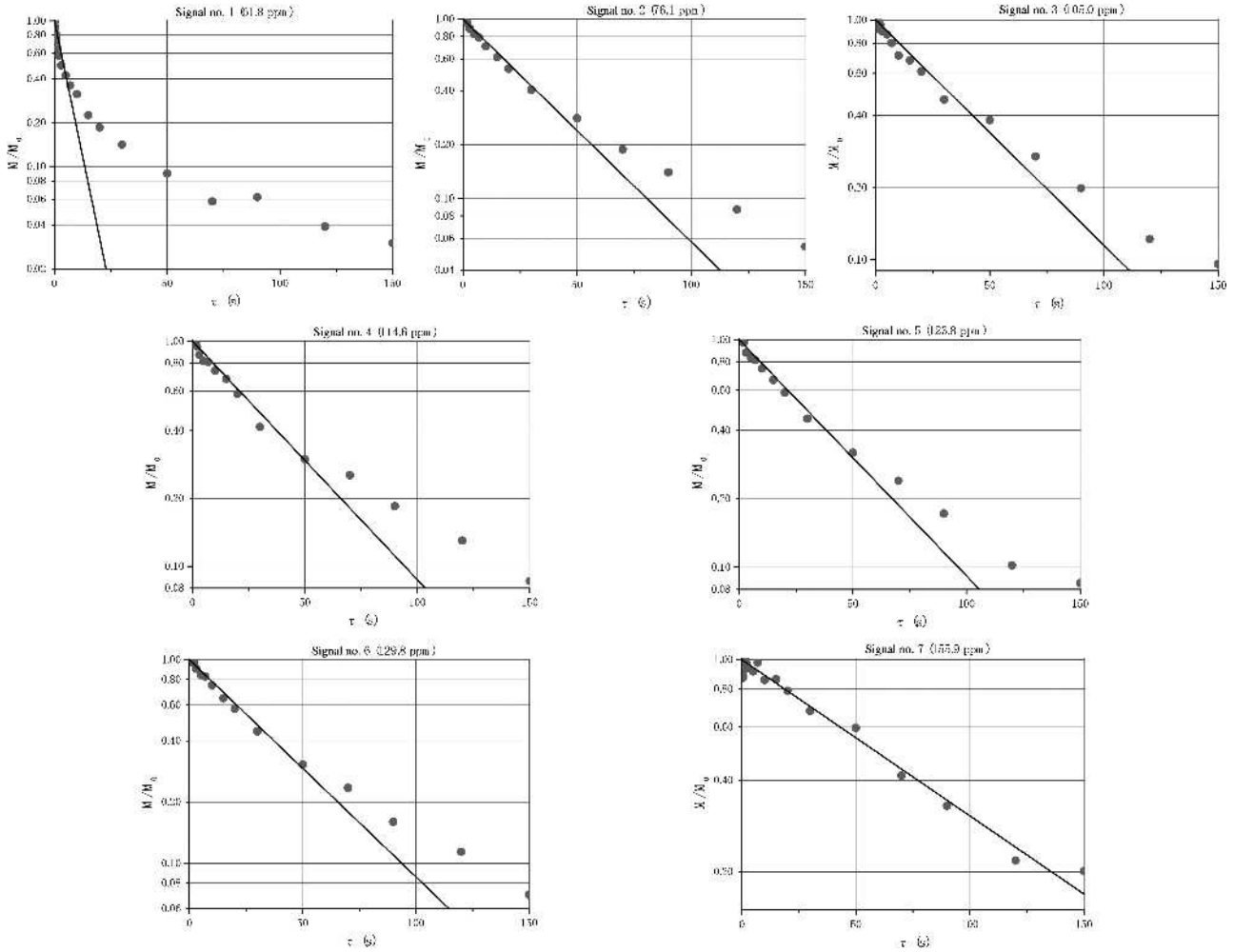

Fig. 6. Relaxation delay time (τ) vs. M_τ/M_0 for amorphous salicin. The solid line is the fit to Eq. (1).

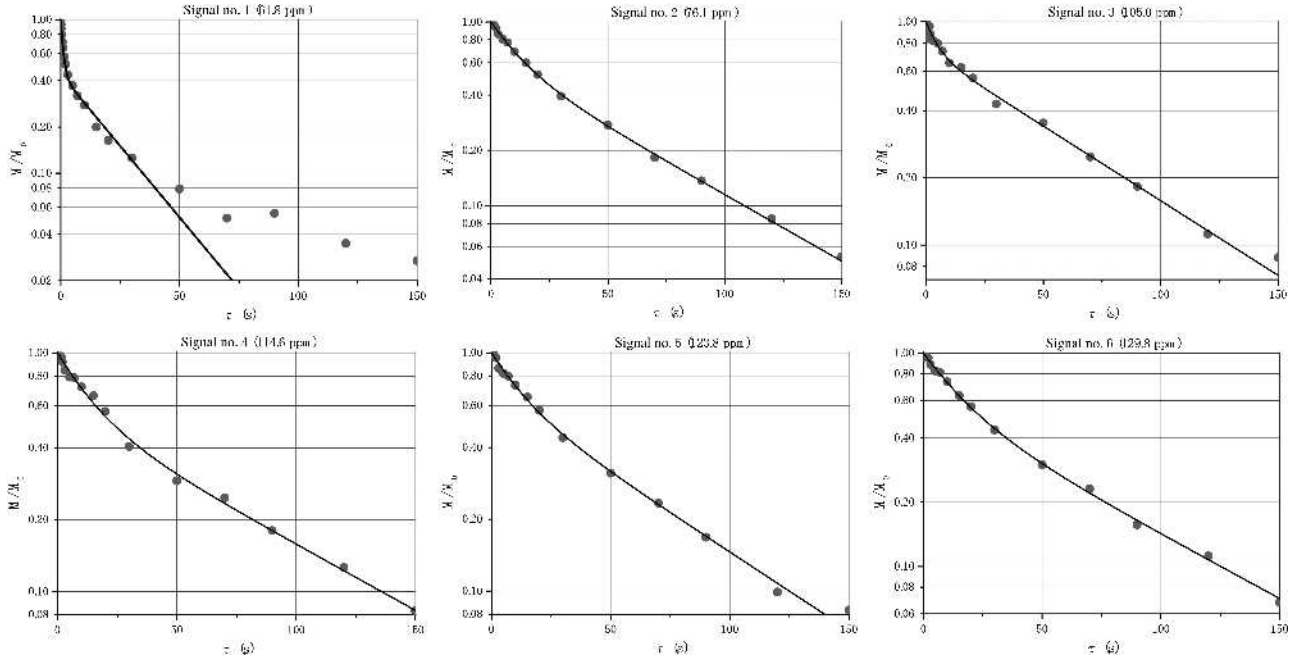

Fig. 7. Relaxation delay time (τ) vs. M_τ/M_0 for signals 1, 2, 3, 4, 5, and 6 of amorphous salicin. The solid line is the fit to Eq. (3).

of each individual carbon. When one signal is attributed to several carbons with multidispersive magnetic relaxation, it should not be fitted to the biphasic model [i.e., signal 1 was attributed to carbon numbers 12 and 13 and was not fitted to Eq. (3)]. Signals 2 and 6 could be fitted to Eq. (3) well, even though they were attributed to multiple carbons. Furthermore, the result that 70% (9/13) of carbons (2–6 and 8–11) had similar T_{1c} values suggested that multidispersive relaxation was not due to individual carbons. These results can be assumed to show that the heterogeneous molecular mobility of amorphous salicin was caused by the heterogeneity of individual structures of the molecule or the existence of different molecules. Signal 7 assigned to carbon number 1 exhibited monodispersive relaxation, and therefore the amorphous salicin molecule as a whole would be homogeneous. The heterogeneous relaxation might be caused by each carbon of the molecule being in different states. The result that the sugar moiety consisting of carbons (8–11) and phenyl carbons (2–6) displayed similar T_{1c} values of 12–16 s suggested that these segments move cooperatively. Moreover, carbon 1 located at the joining of the sugar ring and phenyl ring had the longest T_{1c}, suggesting that molecular mobility resembling a butterfly wing-like movement pattern. Because more than 90% of salicin carbons exhibited shorter T_{1c} in the amorphous state, salicin molecules have high and heterogeneous molecular mobility.

Comparison of the Molecular Mobility of Indomethacin and Salicin

As described in the previous section, our investigation of the molecular mobility of amorphous indomethacin and salicin, measured at 40 K lower than T_g, clarified that the relaxation phenomena of these two molecules differ considerably. In amorphous indomethacin molecules, the indole ring and phenyl ring relax slowly, while the side chains undergo both fast and slow relaxation. As shown in Fig. 8, amorphous indomethacin molecules showed relatively restricted molecular mobility although the side chains exhibited relatively faster local mobility. Seventy-three percent (11/15) of carbons underwent monodispersive relaxation, suggesting that the amorphous state was homogeneous and less mobile, particularly in the backbone structure.

On the other hand, in the amorphous salicin samples, 92% (12/13) of carbons underwent multiphasic relaxation. Each structure of amorphous salicin molecules behaved heterogeneously, indicating that the entire molecule has relatively rapid local mobility as well as slower mobility. Thus, as shown in Fig. 8, it can be concluded that amorphous salicin has higher molecular mobility than amorphous indomethacin has.

Based on the results at same $(T_g - 40)$K measuring temperature, the long T_{1c} of backbone structure of both amorphous indomethacin and salicin had similar values of 76–85 s and 60–84 s, respectively. Except for the methyl group of indomethacin having free rotations, the short T_{1c} of indomethacin was approximately 10s, which was almost the same as the short T_{1c} of salicin. The backbone structure of amorphous indomethacin didn't show the short T_{1c} values (approximately 10 s), while most of carbons of amorphous salicin revealed the short T_{1c} values. In terms of the mobility of the entire molecule, the molecular mobility of the backbone

Fig. 8. Schematic representation of the molecular mobility of amorphous indomethacin (left) and salicin (right). The circles (●) represent carbons showing only slow molecular motion, the solid arrows (↶) represent carbons showing faster local motion, and the dashed arrows (↶) represent carbons that have the potential faster local motion.

structure of indomethacin was more limited than that of salicin, because the shorter T_{1c} implies greater molecular mobility (23).

As shown in Table III, the two molecules differ in their crystallization behavior. There have been various investigations to characterize amorphous indomethacin and salicin. The T_g values of amorphous indomethacin and salicin were reported to be 321 K and 333 K, respectively (2,17,18). Many researchers demonstrated the crystallization of amorphous indomethacin and salicin at temperatures lower than T_g (2,3,7,10,13,17,18). It was also reported that 2 months were required for 60% of pulverized glassy indomethacin samples to crystallize at room temperature (17). However, only 12 days were required for 100% of salicin samples to crystallize at room temperature (18). For comparisons of crystallization behavior, Zhou *et al.* (3) proposed the reduction crystallization temperature, defined as $(T_c - T_g)/(T_m - T_g)$, and data calculated using this formula are shown in Table III. The formula provides a basis for comparing the crystallization behavior of compounds with different T_g values, as a higher reduction crystallization temperature means slower crystallization. The estimated values for amorphous indomethacin and salicin were 0.33 and 0.13, respectively, when the values of T_c, T_g, and T_m for indomethacin were 356, 321, and 428 (2) and the respective values for salicin were 350, 333, and 466 (18). These results confirm that amorphous salicin crystallizes more easily than amorphous indomethacin at room temperature. Thus, it is suggested that the molecular mobility of amorphous pharmaceuticals correlates with their crystallization behavior.

It is reasonable to assume that crystallization from the amorphous state involves nucleation and growth, which are related to molecular mobility. Higher molecular mobility usually means that the molecule is more flexible, which in turn increases the probability of nucleation and growth. It is likely that high molecular mobility induces relocation and rearrangement of molecules and results in nucleation and crystallization. The inhomogeneity of the amorphous structure may also induce nucleation, suggesting that salicin molecules form nuclei easily, and that more mobile molecules crystallize easily.

The differences in the crystallization behavior of indomethacin and salicin are thus attributable to their differing molecular mobility. Amorphous indomethacin molecules move slowly, and thus their crystallization occurs much more slowly than that of amorphous salicin molecules at temperatures lower than T_g. On the other hand, amorphous salicin

Table III. Enthalpy Relaxation Time (τ_{relax}), Glass Transition Temperature, (T_g), Crystallization Temperature (T_c), Melting Temperature (T_m), Reduction Crystallization Temperature, and Percentage of Carbons with Shorter T_{1c} for Amorphous Indomethacin and Salicin

	τ_{relax} at 303 K (h)	T_g (K)	T_c (K)	T_m (K)	Reduction crystallization temperature[1]	Percentage of carbons with shorter T_{1c} (%)
Indomethacin	1	321[2]	356[2]	428[2]	0.33	27
Salicin	30	333[3]	350[3]	466[3]	0.13	92

[1] Reduction crystallization temperature was defined as $(T_c-T_g)/(T_m-T_g)$ in Ref. 3 (D. Zhou *et al. J. Pharm. Sci.,* **91**:1863 (2002)).
[2] Data are quoted from Ref. 2. (M. Yoshioka *et al. J. Pharm. Sci.,* **83**:1700 (1994)).
[3] Data are quoted from Ref. 18. (E. Fukuoka *et al. Chem. Pharm. Bull.,* **37**:1047 (1989)).

molecules have greater mobility, resulting in more rapid crystallization.

CONCLUSIONS

Enthalpic relaxation of amorphous indomethacin occurred more rapidly than that of salicin at temperatures lower than T_g. However, the crystallization rate of indomethacin was slower compared with that of salicin, suggesting that enthalpic relaxation studies alone are not sufficient for the elucidation of physical stability in the amorphous state. We therefore investigated the molecular mobility of amorphous indomethacin and salicin at temperatures below T_g after enthalpic relaxation was complete. The differences in molecular mobility between completely relaxed amorphous indomethacin and salicin were demonstrated based on NMR data. The molecular mobility of the backbone structure of indomethacin was limited, while the side chain showed a higher degree of freedom. Amorphous salicin had relatively higher molecular mobility in each structure of the molecule. This difference in the molecular mobility of the two compounds results in different crystallization behavior. The results of this study also showed that observation of the molecular mobility of individual structures in a molecule in the amorphous state is helpful in the study of crystallization behavior. The experimental results demonstrate that valuable information can be provided by solid-state ^{13}C NMR measurements, which may lead to future optimization of the physical stability of amorphous pharmaceuticals.

REFERENCES

1. L. Yu. Amorphous pharmaceutical solids: preparation, characterization and stabilization. *Adv. Drug Deliv. Rev.* **48**:27–42 (2001).
2. M. Yoshioka, B. C. Hancock, and G. Zografi. Crystallization of indomethacin from the amorphous state below and above its glass transition temperature. *J. Pharm. Sci.* **83**:1700–1705 (1994).
3. D. Zhou, G. G. Z. Zhang, D. Law, D. J. W. Grant, and E. A. Schmitt. Physical stability of amorphous pharmaceuticals: importance of configurational thermodynamic quantities and molecular mobility. *J. Pharm. Sci.* **91**:1863–1872 (2002).
4. J. Liu, D. R. Rigsbee, C. Stotz, and M. J. Pikal. Dynamics of pharmaceutical amorphous solids: the study of enthalpy relaxation by isothermal microcalorimetry. *J. Pharm. Sci.* **91**:1853–1862 (2002).
5. I. Weuts, D. Kempen, K. Six, J. Peeters, G. Verreck, M. Brewster, and G. V. Mooter. Evaluation of different calorimetric methods to determine the glass transition temperature and molecular mobility below T_g for amorphous drugs. *Int. J. Pharm.* **259**:17–25 (2003).
6. S. L. Shamblin, B. C. Hancock, Y. Dupuis, and M. J. Pikal. Interpretation of relaxation time constants for amorphous pharmaceutical systems. *J. Pharm. Sci.* **89**:417–427 (2000).
7. B. C. Hancock and S. L. Shamblin. Molecular mobility of amorphous pharmaceuticals determined using differential scanning calorimetry. *Thermochim. Acta* **380**:95–107 (2001).
8. H. Sillescu. Heterogeneity at the glass transition: a review. *J. Non-Cryst. Solids* **243**:81–108 (1999).
9. P. D. Martino, G. F. Palmieri, and S. Martelli. Molecular mobility of the paracetamol amorphous form. *Chem. Pharm. Bull.* **48**: 1105–1108 (2000).
10. B. C. Hancock, S. L. Shamblin, and G. Zografi. Molecular mobility of amorphous pharmaceutical solids below their glass transition temperatures. *Pharm. Res.* **12**:799–806 (1995).
11. Y. Aso, S. Yoshioka, and S. Kojima. Explanation of the crystallization rate of amorphous nifedipine and phenobarbital from their molecular mobility as measured by ^{13}C nuclear magnetic resonance relaxation time and the relaxation time obtained from the heating rate dependence of the glass transition temperature. *J. Pharm. Sci.* **90**:798–806 (2001).
12. M. D. Ediger, C. A. Angell, and S. R. Nagel. Supercooled liquids and glasses. *J. Phys. Chem.* **100**:13200–13212 (1996).
13. V. Andronis and G. Zografi. Crystal nucleation and growth of indomethacin polymorphs from the amorphous state. *J. Non-Cryst. Solids* **271**:236–248 (2000).
14. K. J. Crowley and G. Zografi. The use of thermal methods for predicting glass-former fragility. *Thermochim. Acta* **380**:79–93 (2001).
15. V. Andronis and G. Zografi. Molecular mobility of supercooled amorphous indomethacin, determined by dynamic mechanical analysis. *Pharm. Res.* **14**:410–414 (1997).
16. Y. Aso, S. Yoshioka, and S. Kojima. Relationship between the crystallization rates of amorphous nifedipine, phenobarbital, and flopropione, and their molecular mobility as measured by their enthalpy relaxation and ^1H NMR relaxation times. *J. Pharm. Sci.* **89**:408–416 (2000).
17. E. Fukuoka, M. Makita, and S. Yamamura. Some physicochemical properties of glassy indomethacin. *Chem. Pharm. Bull.* **34**: 4314–4321 (1986).
18. E. Fukuoka, M. Makita, and S. Yamamura. Glassy state of pharmaceuticals. III. Thermal properties and stability of glassy pharmaceuticals and their binary glass systems. *Chem. Pharm. Bull.* **37**:1047–1050 (1989).
19. A. Koga, E. Yonemochi, M. Machida, Y. Aso, H. Ushio, and K. Terada. Microscopic molecular mobility of amorphous AG-041R measured by solid-state ^{13}C NMR. *Int. J. Pharm.* **275**:73–83 (2004).
20. D. A. Torchia. The measurement of proton-enhanced carbon-13 T_1 values by a method which suppresses artifacts. *J. Magn. Reson.* **30**:613–616 (1978).
21. W. T. Dixon. Spinning-sideband-free NMR spectra. *J. Magn. Reson.* **44**:220–223 (1981).
22. R. I. Shrager. Quadratic programming for nonlinear regression. *Commun. ACM* **15**:41–45 (1972).
23. A. N. Garroway, W. B. Moniz, and H. A. Resing. High resolution ^{13}C nuclear magnetic resonance in cured epoxy polymers. ^{13}C N.M.R. in Polymers. *Chem. Pharm. Bull.* **13**:63–74 (1979).